

METAL ION- PHOSPHATE COMPLEXES: APPLICATIONS IN NANOMEDICINE AND CLINICAL IMPLICATIONS

Julia WERLE¹, Matej FUSEK², Martina STANKOVA², Bozena HOSNEDLOVA², Hoai Viet NGUYEN³, Eva KLAPKOVA¹, Ondrej MITROVSKY¹, Egon WERLE⁴, Richard PRUSA¹, Karel KOTASKA¹, Rene KIZEK^{1,2}

¹*Department of Medical Chemistry and Clinical Biochemistry, Second Faculty of Medicine, Charles University in Prague and Motol University Hospital, V Uvalu 84, 150 06 Prague 5, Czech Republic, EU*

²*Department of Research and Development, EcoNanoLife, 15000 Prague, Czech Republic, EU*

³*Research Center for Environmental Monitoring and Modeling, University of Science, Vietnam National University, 334 Nguyen Trai Street, 100000 Hanoi, Vietnam*

⁴*Department of Medicine I and Clinical Chemistry, Heidelberg University Hospital, 69120 Heidelberg, Germany, EU*

<https://doi.org/10.37904/nanocon.2025.5214>

Abstract

Numerous metal ions are capable of forming nanostructured complexes that may further assemble into micro- and macro-scale architectures. Within biological systems, these structures can lead to significant pathological consequences, including the obstruction of organ excretory pathways or accumulation within body cavities and synovial spaces. Moreover, the formation of such structures has been associated with malignant tumors, highlighting the critical need for systematic investigation in this area. Established methodologies for the synthesis of such nanostructures also offer promising paths for their integration into biomedical applications, such as biosensors and targeted drug delivery systems. For the analytical determination of metal ions within these complexes, a combination of spectrophotometric (UV-Vis, FTIR, AAS) and electrochemical techniques (DPV, CPSA) is employed. The initial identification of these crystalline assemblies typically relies on microscopic visualization. The objective of this study was to synthesize various phosphate-based complexes with selected metal ions and to comprehensively characterize the resulting materials using several analytical techniques, including UV-Vis spectroscopy, Fourier-transform infrared spectroscopy (FTIR), atomic absorption spectroscopy (AAS), electrochemical analysis, and microscopy.

Keywords: FTIR, electrochemistry, crystals, spectroscopy analysis, AAS, nanomedicine, clinical chemistry

1. INTRODUCTION

Phosphates are a class of compounds composed of phosphorus and oxygen, forming a range of different ions, such as H_3PO_4 , H_2PO_4^- , HPO_4^{2-} , and PO_4^{3-} at varying pH. These compounds are well known for forming esters and salts. Inorganic phosphates, as salts of phosphoric acid, may exist as discrete PO_4 units (orthophosphates) or as condensed structures such as pyrophosphates, polyphosphates, and metaphosphates. Calcium phosphates have been extensively studied for various biomedical applications, particularly in dental and orthopedic therapies [1]. Especially calcium phosphate materials are well suited for the design of tissue replacements and tissue repairs. Of particular interest are nanocrystalline inorganic structures such as hydroxyapatite and tricalcium phosphate, owing to their excellent osteoconductivity and biocompatibility [1]. Additionally, they serve as promising drug delivery carriers due to their favorable

biocompatibility, biodegradability, and other advantageous material properties [2]. Notably, the formation of such phosphate-based structures has also been associated with malignant tumor development [3-5].

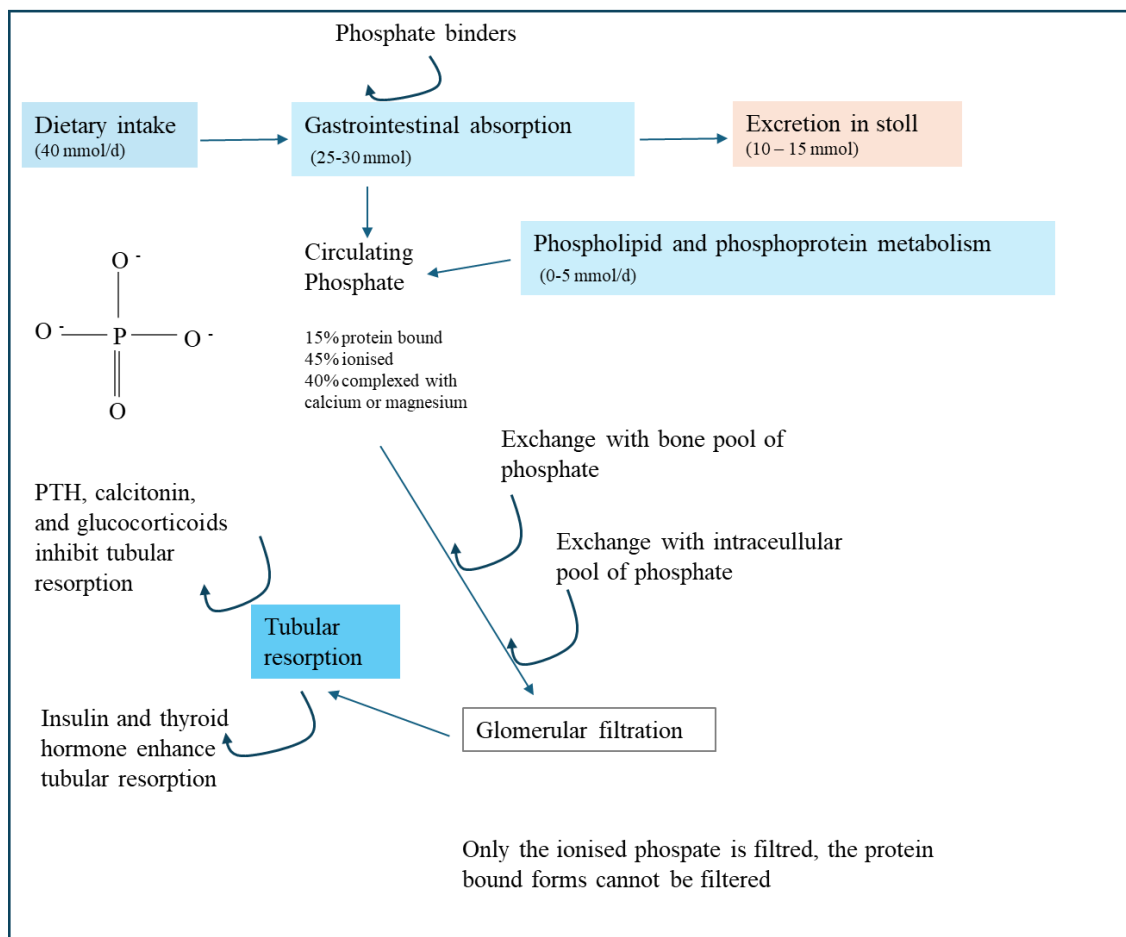


Figure 1 Simplified diagram of the proposed metabolic pathways of phosphate

Furthermore, phosphate groups are integral components of numerous biologically active molecules, including enzymes, nucleic acids, and energetically significant molecules. Their structural versatility enables interactions with a wide range of molecules and ions, forming stable complexes with metals such as calcium and copper. Many of these complexes are capable of crystallizing or forming solid deposits within living organisms, potentially leading to clinically significant pathologies such as calcifications and lithiasis that often require medical intervention. For instance, calcium pyrophosphate can form crystals that frequently deposit in joints, triggering inflammatory responses [2]. Consequently, research in this field can provide significant information for the development of novel therapeutic strategies. Nanoparticles of phosphate complexes can be synthesized using microwave-assisted methods, yielding stable structures [6], and may also enhance technological processes [7]. Additionally, these molecules can improve the functional properties of other nanomaterials and are thus of growing interest in sensor development. Their ability to interact selectively with metal ions also positions them as promising candidates for targeted detection systems [8]. To analyze biological aggregates or concrements (e.g., pathological stones), techniques such as scanning electron microscopy (SEM), Fourier-transform infrared spectroscopy (FTIR), and X-ray diffraction (XRD) are commonly employed [9]. Moreover, the monitoring of molecular interactions can be effectively performed using spectrophotometric or electrochemical techniques due to their simplicity and accessibility. In our preliminary experiments, the behavior of selected pyrophosphate compounds was investigated [10]. The primary objective of this study was to analyze a series of phosphate-based complexes with potential clinical relevance.

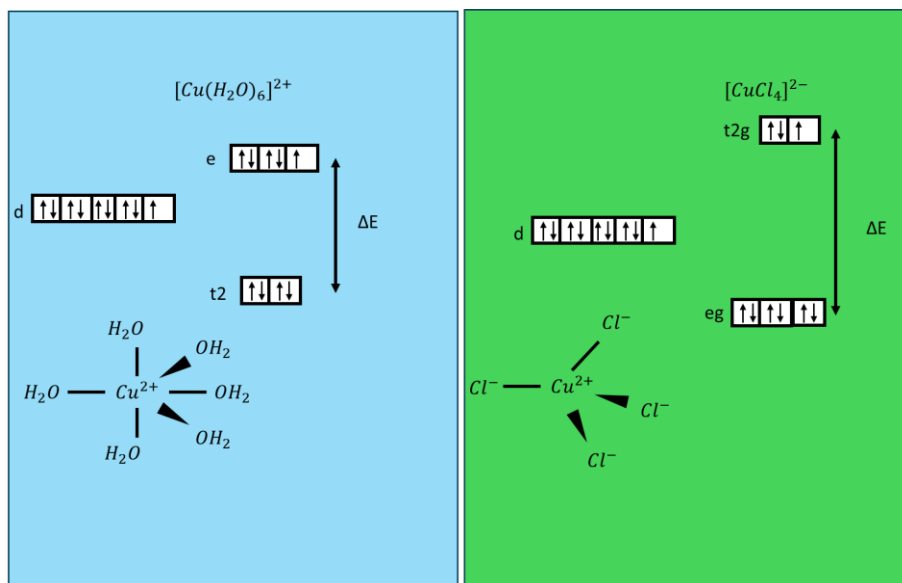


Figure 2 Simplified diagram of the proposed metabolic pathways of phosphate

2. MATERIAL AND METHODS

2.1. Material and chemicals

The analytical grade chemicals (ACS) used were purchased from Sigma Aldrich (St. Louis, MO, USA): NaH_2PO_4 , Na_2HPO_4 , Na_3PO_4 , KCl, NaCl, NaOH, HCl. The disposable plastic tips and microtubes used were of RNA and DNA free quality (Eppendorf, Germany). Disposable 1 cm UV-Vis cuvettes for the single-beam spectrophotometer were purchased from VWR (USA). Deionized water was prepared using reverse osmosis equipment Aqual 25 (AQUAL s.r.o., Brno, Czech Republic) and subsequently treated to an 18 M Ω purity by an ELGA deionizer from Purelab Flex (London, UK). Conductivity and pH were measured with a MU 6100L multimeter from VWR (Radnor, PA, USA). The pH-electrode (662-1161 Phenomenex pH electrode pH 0–14/3M KCl, Torrance, USA) was regularly calibrated with two-point calibration (VWR buffers, at 25 °C).

2.2. UV-Vis spectroscopy

Spectrophotometric measurements were conducted using a UV-3100 PC spectrophotometer (VWR, USA). For these measurements, plastic cuvettes (UV-Vis, BRAND, USA) were utilized. 500 μ L reagent was pipetted into the cuvette followed by 100 μ L of sample. The reaction solution was used as blank. Further spectrophotometric analyses were performed on a polystyrene microtiter plate, which had been pre-washed with 18 M Ω water (3 times, 300 μ L) at room temperature using a reader (TECAN, Switzerland). 50 μ L of sample and 250 μ L of reagent were pipetted. Absorbance measurements were taken every minute at 540 nm over a period of 60 minutes. The analysis was conducted using the VARIOSKAN Lux multimode reader (Thermo Scientific, USA). The scanning was performed across a wavelength range of 300 to 800 nm, with 1 nm increments. Data control and collection were managed using the SKANIT RE software (version 6.0.1).

2.3. Fourier-Transform Infrared (FTIR) Spectroscopy

All samples were dehumidified (ECOCELL BMT, Czechia, 130 °C, 24 h) and maintained in a desiccator (silica gel) prior to analysis. The functional group modifications of the samples were characterized using Fourier-transform infrared spectroscopy (Nicolet iS10 Spectrometer) by the potassium bromide (KBr) pellet method. The dried samples (30 mg) were mixed with KBr (500 mg) and pressed under mechanical pressure in mortar

(5 min). Spectra were recorded between the wavenumber range of 4000 and 400 cm^{-1} . Software was used to remove noise and smoothing utilizing Savitsky-Golay filter, baseline correction and Fourier transformation.

2.4. Automated analysis

For the chemical analysis of specimens, the Atellica Solutions CH 930 analyser (Siemens, USA) was used for photometric analyses. The urine sediment was analysed using Atellica 1500, which combines the Clinitek Novus analyser and the Atellica Automated Urinalysis System 800 (Siemens, USA). The semi-automated Aution Eleven AE-4020 (Arkray, Japan) with Aution Sticks 10EA was utilized for the chemical urine analysis with a measurement principle of test strip method and dual-wavelength reflection photometric method. For the detection of ions, an integrated multisensor technology (IMT) on printed electrodes was employed. Osmolality was measured using the OsmoPRO osmometer (Advanced Instruments, USA).

2.5. Electrochemical analysis

Electrochemical measurements were performed with an AUTOLAB Analyser (Metrohm, Herisau, Switzerland) connected to VA-Stand 663 (Metrohm, Herisau, Switzerland), using a standard cell with three electrodes. The working electrode was a hanging mercury drop electrode (HMDE) with a drop area of 0.4 mm^2 . The reference electrode was an Ag/AgCl/3M KCl electrode, and the auxiliary electrode was a graphite electrode. The supporting electrolyte was prepared by mixing buffer components. The samples analyzed by differential pulse voltammetry (DPV) were deoxygenated prior to measurements by purging with argon (99.999%) saturated with water for 20 s. In our studies, the Brdicka supporting electrolyte contained 1 mM $\text{Co}(\text{NH}_3)_6\text{Cl}_3$, 1 M $\text{NH}_3(\text{aq})$, and 1 M NH_4Cl , pH = 9.6; a surface-active agent was not added. The DPV Brdicka reaction parameters were as follows: an initial potential of -0.6 V, an end potential of -1.85 V, a modulation time of 0.057 s, an interval of 0.2 s, a step potential of 1.05 mV/s, a modulation amplitude of 250 mV, and accumulation time of 240 s [11, 12].

2.6. Microscopy

Microscopic analysis was performed on an OLYMPUS BX53 microscope paired with a CANON camera and an evaluation program (QuickPHOTO CAMERA 3.2). Dry urine sample (1 mg) was used on a glass slide after intensive grinding. For each magnification (100, 200, 400, and 600 times), ten images were evaluated in both transmitted and polarized lighting. Selected images were recorded in the evaluation program and saved.

2.7. Data treatment and descriptive statistics

The experimental work was carried out in three independent experiments. The analysis of each sample was carried out 5 times. The obtained data are presented as average values. From the proposed study no experimental subjects were excluded from the proposed experimental studies. All the obtained data were stored in the QINSLAB database (Czech Republic). When possible, data was processed and evaluated mathematically and statistically in the QINSLAB database. The exclusion of outliers in the data sets was performed by calculating the Grubbs test. Photographs were processed by programme ColorTest, which assigns intensity to the individual pixels of the studied image in the colour area. For the publication purpose, data were processed using Microsoft (USA).

3. RESULTS AND DISCUSSION

The crystallization process resulted in well-defined crystals of the individual molecules under investigation namely, pyrophosphate, Cu-pyrophosphate, and Ca-pyrophosphate. These crystals were subsequently examined using light and polarization microscopy. The particle sizes ranged between 300 and 800 nm, which can be attributed to potential nanoparticle aggregation [13]. A critical parameter is the calcium-to-phosphate (Ca/P) molar ratio. Depending on the reaction conditions and stoichiometry, various crystalline products may

form, including $(\text{Ca}^{2+})_{10}(\text{PO}_4^{3-})_6(\text{OH})_2$; $(\text{Ca}^{2+})_3(\text{PO}_4^{3-})_2$; $(\text{Ca}^{2+})_8(\text{PO}_4^{3-})_6(\text{H}^+)_2$; $(\text{Ca}^{2+})(\text{HPO}_4^{3-})$ [13]. The structure of apatite is highly flexible, accommodating various ionic substitutions [14]. Hydroxyapatite $(\text{Ca}_{10}(\text{PO}_4)_6(\text{OH})_2)$ contains active functional groups that can be substituted by other cations or anions. Previous studies have demonstrated successful functionalization of hydroxyapatite with a range of metal ions, including copper [15], zinc [16, 17], gold [18], and silver [19]. These interactions are of particular interest in biomedical applications. For instance, zinc-substituted apatites have been shown to enhance bone regeneration through prolonged ion release. The presence of zinc ions could stimulate bone mineralization, promote protein synthesis, and support the structural and functional integrity of cellular membranes. Likewise, copper ions possess notable antibacterial properties and can be incorporated into phosphate structures to impart bioactivity [20]. Crystallization was carried out under aqueous, acidic, and basic conditions, leading to the formation of various crystal morphologies. Selected crystalline products were analyzed using both bright-field and polarized light microscopy. Polarization microscopy revealed anisotropic, acicular crystals with distinct linear growth features along their margins.

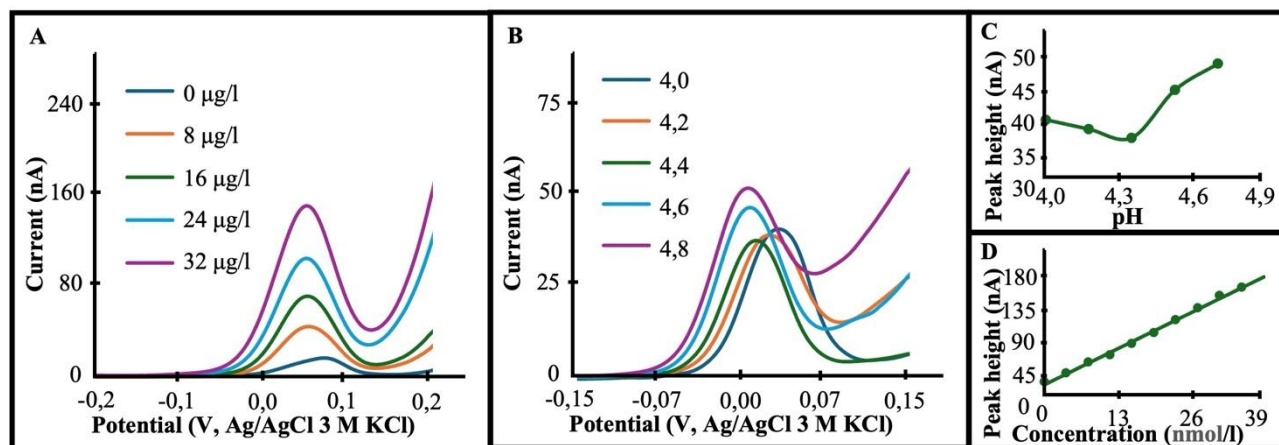


Figure 3 Electrochemical study of copper pyrophosphate in acetate buffer. (A) Typical voltammogram of copper phosphate ($c = 12 \text{ nmol/l}$) at different pH (4,0-4,8) and variation of (B) peak height and (C) peak potential

The signals of the synthesized complexes were analyzed using Fourier-transform infrared (FTIR) spectroscopy to enhance spectral resolution [21]. FTIR analysis was applied specifically to phosphate compounds, with particular attention given to calcium phosphates as detailed in reference [21]. FTIR spectra revealed a characteristic absorption band for pyrophosphate in the region of $930\text{--}940 \text{ cm}^{-1}$, with a distinct maximum at 930 cm^{-1} . Additionally, the region between $1200\text{--}1140 \text{ cm}^{-1}$ was identified to be specific for sulphate. Furthermore, UV-Vis spectroscopy was employed to characterize the individual complexes. Depending on the pH, the formation of various complex species was presumed: $(\text{H}_3\text{P}_2\text{O}_7)^-$ exhibited absorption maxima within the $250\text{--}330 \text{ nm}$ range; $(\text{CuCl}_4)^{2-}$ showed maxima in the $350\text{--}500 \text{ nm}$ region; and $(\text{Cu}(\text{H}_2\text{O})_6)^{2+}$ demonstrated absorptions in the $750\text{--}850 \text{ nm}$ range. Electrochemical analysis was carried out in a 0.1 M acetate buffer at pH 5 under previously optimized conditions [10]. For comparison, 0.1 M CuCl_2 was first analyzed with correlation to accumulation time and preconcentration potential, which was set at -1.2 V . The current response exhibited a linear dependence on accumulation time ($0\text{--}300 \text{ s}$), described by the equation $y = 0.39x$, with a correlation coefficient of $r = 0.99$. Maximum signal intensity was observed at approximately 240 seconds. A characteristic redox signal for copper ions was observed at a potential of $0.15 \pm 0.01 \text{ V}$ ($n = 5$; $\text{RSD} = 1.5\%$). A strictly linear relationship between copper ion concentration and current response was obtained ($y = 1.88x$; $r = 0.999$, $n = 8$), with a LOD of 1.9 nM , a LOQ of 6.4 nM , and a RSD of 5.6% . Inter-day reproducibility was within 5% . Subsequently, the synthesized phosphate–metal complexes were analyzed. Upon complexation with copper ions, distinct redox signals were observed at three key potentials: peak A at $-0.30 \pm 0.03 \text{ V}$, peak

B at -0.05 ± 0.01 V, and peak C at 0.11 ± 0.02 V. The proposed analytical methodology was applied to the analysis of real samples of crystals and stones. One such analysis was performed on a pyrophosphate-based stone obtained from a pediatric patient, with a phosphate/creatinine ratio of 2.31 and 1.65 mmol/mmol (reference range < 2.70 mmol/mmol).

4. CONCLUSION

Phosphate structures containing metal ions were studied due to their dual significance: they possess potential for nanomedicine applications, yet they can also form spontaneously within organisms, contributing to a range of serious health conditions. In some cases, their presence has been associated with malignant diseases. However, current knowledge regarding their formation and behavior in biological systems remains limited. In this study, investigated the formation and behavior of pyrophosphate complexes with various metal ions was investigated. The formation and characterization of such complexes represent a considerable scientific challenge due to their structural diversity and dynamic interactions. To analyze these phosphate - metal ion complexes, a combination of spectrophotometric and electrochemical techniques was employed.

ACKNOWLEDGEMENTS

The project is being implemented under the grant project Liga proti rakovině Praha.

REFERENCES

- [1] VECBISKENA, L., DE NARDO, L., CHIESA, R. 2014. Nanostructured Calcium Phosphates for Biomedical Applications. 22nd International Baltic Conference on Engineering Materials & Tribology (BALTMATTRIB), Nov 14-15 2013 Riga, LATVIA. 212-+.
- [2] BASSETT, D. C., ROBINSON, T. E., HILL, R. J., GROVER, L. M., BARRALET, J. E. Self-assembled calcium pyrophosphate nanostructures for targeted molecular delivery. *Biomaterials Advances*, 2022, vol. 140, no. pp. 213086.
- [3] WAN, Y., ZHANG, J. Q., CHEN, M., MA, M., SHENG, B. W. Elevated serum triglyceride levels may be a key independent predicting factor for gallbladder cancer risk in gallbladder stone disease patients: a case-control study. *Bmc Endocrine Disorders*, 2022, vol. 22, no. 1, pp.
- [4] PEERAPEN, P., BOONMARK, W., PUTPEERAWIT, P., THONGBOONKERD, V. Calcium oxalate crystals trigger epithelial-mesenchymal transition and carcinogenic features in renal cells: a crossroad between kidney stone disease and renal cancer. *Experimental Hematology & Oncology*, 2022, vol. 11, no. 1, pp.
- [5] SAWAYA, M., CORDINA-DUVERGER, E., LAMY, P. J., TRÉTARRE, B., MENEGAUX, F. Kidney and gallbladder stones and the risk of prostate cancer: Results from the EPICAP study. *Plos One*, 2025, vol. 20, no. 1, pp.
- [6] APSANA, G., GEORGE, P. P., DEVANNA, N. Facile green synthesis and characterization of calcium pyrophosphate nanoparticles using D-Glucose. *Materials Today: Proceedings*, 2017, vol. 4, no. 10, pp. 10913-10920.
- [7] CESIULIS, H., BUDREIKA, A. Electroreduction of Ni (II) and Co (II) from Pyrophosphate solutions. *Materials Science (Medziagotyra)*, 2010, vol. 16, no. 1, pp. 52-56.
- [8] LI, J., WANG, Z., YIN, H., LV, S., WANG, Y., ZHANG, J., GUO, P., LI, D. Terpyridine functionalized gold nanoparticles: Assembling induced by metal ions and subsequent disassembly by pyrophosphate. *Colloids and Surfaces A: Physicochemical and Engineering Aspects*, 2025, vol. 719, no. pp. 136948.
- [9] BOUHA, M., ECHAJIA, M., AMINI, L., MBARKI, M., ELHADIRI, N., OUBENALI, M., BERKANI, M. Chemical Composition Analysis of Human Gallstones in Beni Mellal-Khenifra, Morocco. *Brazilian Journal of Analytical Chemistry*, 2025, vol. 12, no. 46, pp. 92-103.
- [10] KOTASKA, K., WERLE, J., FUSEK, M., HOAI, N. V., CEPOVA, J., FOROTVA, M., KLAPKOVA, E., PRUSA, R., KIZEK, R. SPECTROPHOTOMETRIC AND ELECTROCHEMICAL ANALYSIS OF METAL IONS PHOSPHATATE COMPLEXES. *Clin Chem Lab Med*, 2025, vol. 63, no. Special Suppl, pp. S1775-S1775.

- [11] PETRLOVA, J., POTESIL, D., MIKELOVA, R., BLASTIK, O., ADAM, V., TRNKOVA, L., JELEN, F., PRUSA, R., KUKACKA, J., KIZEK, R. Attomole voltammetric determination of metallothionein. *Electrochim. Acta*, 2006, vol. 51, no. 24, pp. 5112-5119.
- [12] MELICH, L., FORTOVA, M., HOSNEDLOVA, B., PODHAJSKY, J., RYCHLY, O., WERLE, J., BURESOVA, K., DUNOVSKA, K., VYSLOUZILOVA, L., KLAPKOVA, E., KOTASKA, K., CEPOVA, J., JEDLICKOVA, B., STEPANKOVA, O., PRUSA, R., KIZEK, R. Studium hladiny metalothioneinu v séru pacientů se zhoubným nádorem. *Chem. Listy*, 2023, vol. 117, no. 9, pp. 573-580.
- [13] SUN, L. M., CHOW, L. C., FRUKHTBEYN, S. A., BONEVICH, J. E. Preparation and Properties of Nanoparticles of Calcium Phosphates With Various Ca/P Ratios. *Journal of Research of the National Institute of Standards and Technology*, 2010, vol. 115, no. 4, pp. 243-255.
- [14] ROGOJAN, R., ANDRONESCU, E., DINU, E., GHEORGHE, S. Nanostructure processing of calcium phosphates doped with zinc ions. *Journal of Optoelectronics and Advanced Materials*, 2015, vol. 17, no. 5-6, pp. 884-888.
- [15] FERNANE, F., MECHERRI, M. O., SHARROCK, P., FIALLO, M., SIPOS, R. Hydroxyapatite interactions with copper complexes. *Materials Science & Engineering C-Materials for Biological Applications*, 2010, vol. 30, no. 7, pp. 1060-1064.
- [16] IQBAL, N., KADIR, M. R. A., MAHMOOD, N. H., SALIM, N., FROEMMING, G. R. A., BALAJI, H. R., KAMARUL, T. Characterization, antibacterial and in vitro compatibility of zinc-silver doped hydroxyapatite nanoparticles prepared through microwave synthesis. *Ceramics International*, 2014, vol. 40, no. 3, pp. 4507-4513.
- [17] REN, F., XIN, R., GE, X., LENG, Y. Characterization and structural analysis of zinc-substituted hydroxyapatites. *Acta Biomaterialia*, 2009, vol. 5, no. 8, pp. 3141-3149.
- [18] DOMÍNGUEZ, M. I., ROMERO-SARRIA, F., CENTENO, M. A., ODRIÓZOLA, J. A. Gold/hydroxyapatite catalysts Synthesis, characterization and catalytic activity to CO oxidation. *Applied Catalysis B-Environmental*, 2009, vol. 87, no. 3-4, pp. 245-251.
- [19] CIOBANU, C. S., MASSUYEAU, F., CONSTANTIN, L. V., PREDOI, D. Structural and physical properties of antibacterial Ag-doped nano-hydroxyapatite synthesized at 100°C. *Nanoscale Research Letters*, 2011, vol. 6, no. 1, pp. 613.
- [20] ELBASHIR, S., SALH, R., ANDERSSON, B. M. New insights into structural and spectroscopic characteristics of Cu²⁺-doped (3-Ca₃(PO₄)₂): Correlation between Cu²⁺-concentration and material properties. *Materials & Design*, 2025, vol. 252, no. pp.
- [21] BERZINA-CIMDINA, L., BORODAJENKO, N. 2012. Research of Calcium Phosphates Using Fourier Transform Infrared Spectroscopy. In: THEOPHANIDES, T. (ed.) *Infrared Spectroscopy - Materials Science, Engineering and Technology*. Rijeka: IntechOpen.